

2 **Microdevices for extensional rheometry of low viscosity**
3 **elastic liquids: a review**

4 **F. J. Galindo-Rosales · M. A. Alves ·**
5 **M. S. N. Oliveira**

6 Received: 15 March 2012 / Accepted: 27 June 2012
7 © Springer-Verlag 2012

8 **Abstract** Extensional flows and the underlying stability/
9 instability mechanisms are of extreme relevance to the
10 efficient operation of inkjet printing, coating processes and
11 drug delivery systems, as well as for the generation of
12 micro droplets. The development of an extensional rheo-
13 meter to characterize the extensional properties of low
14 viscosity fluids has therefore stimulated great interest of
15 researchers, particularly in the last decade. Microfluidics
16 has proven to be an extraordinary working platform and
17 different configurations of potential extensional microrheo-
18 meters have been proposed. In this review, we present an
19 overview of several successful designs, together with a
20 critical assessment of their capabilities and limitations.

21
22 **Keywords** Extensional flow · Filament stretching ·
23 Filament thinning · Diluted polymer solution · Rheometry ·
24 Microfluidics · Extensional viscosity · Viscoelasticity

25 **1 Introduction**

26 Extensional deformation plays a significant role in many
27 processing operations of polymer melts and solutions.
28 Examples include extrusion, coating flows, contraction
29 flows, fiber spinning, blow molding, film blowing, and foam

30 production (Gaudet and McKinley 1998; Zheng et al.
31 2011). Since extensional flows strongly orient polymer
32 molecules and asymmetric particles, the presence of regions
33 of strong extensional flow in processing operations can have
34 a major effect on final product properties (Macosko 1994).
35 Moreover, in the food industry, the extensional properties
36 are also important in various stages of the product life cycle,
37 from the initial stage of formulation and process design, to
38 process and quality control of products, to the final stage
39 of sensory perception of the product by the consumer
40 (Padmanabhan and Bhattacharya 1993; Padmanabhan
41 1995; Funami 2011). There are also other industrial and
42 commercial applications, such as agrochemical spraying,
43 inkjet printing, turbulent drag reduction or enhanced oil
44 recovery, in which the extensional properties of the working
45 fluids are of extreme importance (Oliveira et al. 2006;
46 Rothstein 2008), since viscoelastic fluids frequently exhibit
47 strong extensional thickening well beyond the Trouton ratio
48 (Trouton 1906) found for Newtonian fluids ($Tr = \eta_e/\eta = 3$
49 for axisymmetric elongation, or $Tr = \eta_e/\eta = 4$ for planar
50 elongation). Therefore, in order to accurately model these
51 materials, detect subtle dissimilarities in their composition,
52 and to describe or predict the processing conditions that will
53 optimize fluid flow or characteristics of the final product, a
54 thorough rheological characterization of materials in both
55 shear and extensional flow conditions is recommended
56 (Barnes et al. 1993).

57 Despite the recognized importance of extensional flows,
58 we still face an unbalanced scenario in the field of rheo-
59 metry, with the rheological characterization under simple
60 shear flow being by far the most abundant in rheology, to
61 such an extent that it often becomes a synonym for rheo-
62 logy in general (Dukhin and Zelenev 2010). However, it
63 is not possible to describe adequately the highly complex
64 dependency on both strain and strain rate experienced by a

A1 F. J. Galindo-Rosales (✉) · M. A. Alves
A2 Departamento de Engenharia Química, Centro de Estudos
A3 de Fenómenos de Transporte (CEFT), Faculdade de Engenharia
A4 da Universidade do Porto, Rua Dr. Roberto Frias s/n,
A5 4200-465 Porto, Portugal
A6 e-mail: galindo@fe.up.pt; curro@galindorosales.com

A7 M. S. N. Oliveira
A8 Department of Mechanical and Aerospace Engineering,
A9 University of Strathclyde, Glasgow G1 1XJ, UK

fluid element of a viscoelastic material in a strong extensional flow using exclusively a shear rheological characterization. This has been the motivation which has been fueling extensive research in the past decades to understand the extensional flow behavior of different materials. Research in this topic has involved a synergistic effort in theoretical analysis of extensional flow behavior in order to determine the critical parameters and identify the optimal flow kinematics, and in improving the experimental design of extensional rheometers in order to successfully impose the desired kinematics (Nijenhuis et al. 2007). Ideally, a pure extensional (or shear-free) flow, in which the rate-of-strain tensor ($\mathbf{D} = \frac{1}{2}[\nabla\mathbf{v} + \nabla\mathbf{v}^T]$) has only non-zero values on the diagonal elements ($\frac{\partial u_i}{\partial x_j} = 0, \forall i \neq j$) and consequently the vorticity tensor is null ($\mathbf{w} = \frac{1}{2}[\nabla\mathbf{v} - \nabla\mathbf{v}^T] = \mathbf{0}$), would allow us to characterize properly the extensional properties of the fluid. However, due to difficulties associated with imposing purely extensional deformations, the development of instrumentation able to carry out extensional viscosity measurements is still a challenging task. Twenty five years ago, Bird et al. (1987) summarized this idea in the following statement: "Unlike the situation for shear flows where there are numerous methods available for measuring material functions of a wide variety of polymeric liquids, techniques for measuring the kinds of shear-free flow material functions have been developed only for polymer melts and high-viscosity solutions". In spite of the difficulties in generating homogeneous extensional flows, avoiding shear components and controlling the strain history of the material elements (Petrie 1997; Anna et al.

2001; Ríos et al. 2002; Bänsch et al. 2004), especially with low viscosity liquids, significant improvements have been achieved over the last 25 years. As a consequence of this active research, a family of extensional rheometers and detachable extensional rheometer fixtures for use in commercial torsional rheometers are nowadays available on the market and allow the user to cover a wide range of materials from low to highly viscous fluids, and from polymer solutions to polymer melts, as schematically illustrated in Fig. 1. Most of the apparatus developed for measuring the extensional viscosity are more appropriate for high-viscosity materials, such as polymer melts (Münstedt 1979; Meissner 1985a, b; Maia et al. 1999; Schweizer 2000; Sentmanat et al. 2005; Göttfert 2011; Franck 2011), mainly due to the fact that the high viscosity of such polymer melts allows the preparation of homogeneous sheets or rods of material that are subsequently subjected to an elongation process under conditions of either constant deformation rate or constant stress (McKinley and Sridhar 2002). On the other hand, methods for determining the extensional properties of less viscous complex fluids, such as dilute polymer solutions, are more limited and in most cases are still under active development.

The opposed jet rheometer developed by Fuller et al. (1987), commercialized as the RFX instrument by Rheometrics (now TA Instruments), was able to characterize the extensional properties of low viscosity fluids. This technique was used extensively to measure the extensional properties of various aqueous solutions in the 1990s (e.g. Hermansky and Boger 1995; Ng et al. 1996). However, since large deformation rates were required to induce

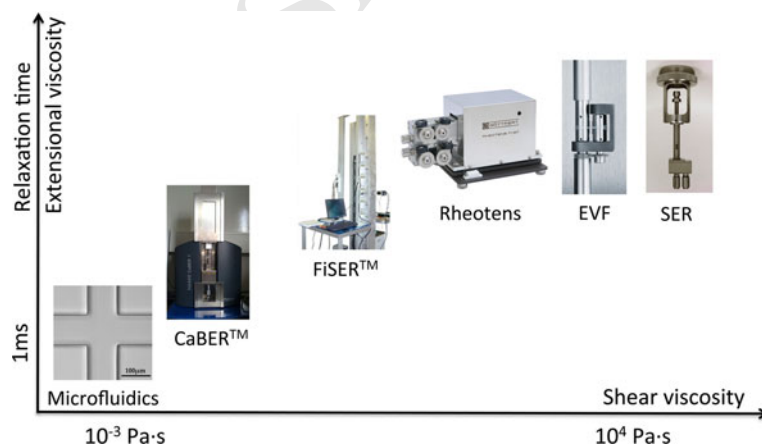


Fig. 1 Range of available extensional rheometers: operability diagram in terms of the fluid shear viscosity and extensional viscosity (or shear viscosity and relaxation time) of the materials that are typically measured. The CaBERTM device was developed by the Cambridge Polymer Group (MA, USA) and is commercialized by ThermoFischer (MA, USA). The FiSERTM device illustrated was developed and commercialized by the Cambridge Polymer Group. The Rheotens 71.97 device illustrated is commercialized by Göttfert (Germany).

The extensional viscosity fixture (EVF) is commercialized by TA Instruments (DE, USA). The Sentmanat Extensional Rheometer (SER) fixture was developed by Dr. M. Sentmanat and is commercialized by Xpansion Instruments (OH, USA) and likewise the EVF can be used as a detachable fixture on a commercial rotational rheometer. The images of FiSERTM, Rheotens, EVF and SER are reproduced with permission of Cambridge Polymer Group, Göttfert, TA Instruments and Xpansion Instruments, respectively.

126 significant viscoelastic effects, the inertial stresses in the
 127 fluid at such rates can completely mask the viscoelastic
 128 stresses resulting from molecular deformation, leading to
 129 erroneous results (Dontula et al. 1997; Rodd et al. 2005b).
 130 Nevertheless, although the RFX instrument is nowadays
 131 out of the market as a standalone device, it is still a subject
 132 of research and recently a new opposed-nozzle fixture, that
 133 can be mounted onto a controlled strain rheometer, was
 134 developed by Soulages et al. (2009a).

135 Among the plethora of techniques developed for
 136 extensional characterization of mobile liquids, reviewed by
 137 Gupta and Sridhar (1988) and McKinley and Sridhar
 138 (2002), filament stretching rheometry has sparked off great
 139 interest since the pioneering work of Matta and Tytus
 140 (1990) and Bazilevsky et al. (1990). In just one decade it
 141 matured to such an extent that in 2001 it was already
 142 considered as an accurate method for characterizing the
 143 response of viscoelastic fluids and, in particular, of viscous
 144 dilute polymer solutions, almost achieving an ideal uni-
 145 axial extensional deformation (Anna et al. 2001). According
 146 to Sridhar (2000) it represented the culmination of
 147 about four decades of intense research in the development
 148 of a suitable extensional rheometer. A major advantage is
 149 that the velocity field far from the rigid endplates is
 150 essentially one-dimensional and purely extensional
 151 (Schultz and Davis 1982). Over the past two decades different
 152 filament stretching configurations have been proposed
 153 for generating such flows, but two among those have
 154 showed enhanced performance for rheometric purposes
 155 (McKinley et al. 2001):

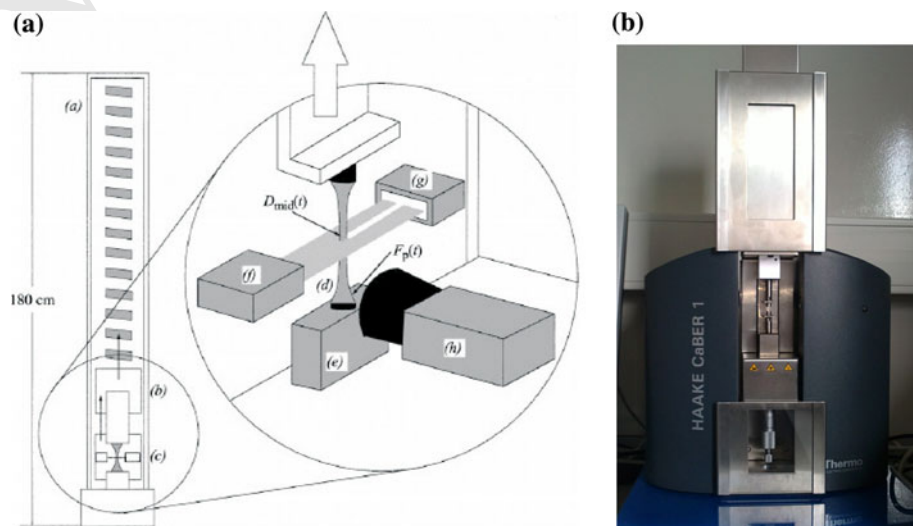
- 156 • The filament stretching extensional rheometer (FiS-
 157 ER™) illustrated in Fig. 2a imposes an exponential
 158 velocity to the upper plate in order to induce a uniaxial
 159 extensional flow with constant strain rate, rather than
 160 constant tensile force, as in the original concept of

Matta and Tytus (1990). The temporal evolution of the tensile force exerted by the fluid column on the bottom endplate and of the filament radius at the axial mid-plane of the filament are both measured and used to compute the transient extensional viscosity (McKinley et al. 2001). A more reliable version of the FiSER™ can use a real-time algorithm to control the upper plate velocity in order to achieve the desired exponential decay of the filament diameter at the midpoint (Anna et al. 1999).

- 161 • The capillary breakup extensional rheometer (CaBER™), based on the ideas of Bazilevsky et al.
 162 (1990), imposes an extensional step strain of order
 163 unity and the filament subsequently thins under the
 164 influence of capillary forces without additional kinematic
 165 input at the boundaries. Subsequently, the fluid
 166 filament undergoes a thinning process with an exten-
 167 sional strain rate defined by the extensional properties
 168 of the fluid. Large extensional strains can still be
 169 attained as the mid-region of the filament progressively
 170 necks down and eventually breaks. Typically, the only
 171 measured quantity is the time evolution of the midpoint
 172 diameter of the necking filament (see Fig. 2b) and the
 173 relaxation time is determined from the exponential
 174 decay of the filament diameter with time (McKinley
 175 et al. 2001).

The relative merits of the CaBER™ and FiSER™ apparatuses, as well as the dynamics of capillary thinning of Newtonian and non-Newtonian fluids have been discussed thoroughly by McKinley and Tripathi (2000), McKinley and Sridhar (2002) and McKinley (2005). Even though the CaBER™ can be used to measure relaxation times of viscoelastic liquids with significantly lower viscosities than the FiSER™ there is still a limit of operation,

Fig. 2 **a** Schematic diagram of a FiSER™ for moderately viscous materials [reprinted from Anna et al. (1999), Copyright (1999), with permission from Elsevier Science]. **b** Commercial CaBER™ 1 apparatus



as depicted in the CaBER™ operability diagram presented by Rodd et al. (2005b). This diagram defines a minimum limit for the measurable relaxation time around 1 ms for liquids with a shear viscosity of about 3 mPa s achievable by selecting appropriately the operating conditions, which in practical terms is very difficult to achieve due to strong inertial effects and the fact that the position of the narrowest part of the filament is not always matching the position of the laser micrometer. For these reasons, the use of high speed cameras for recording the filament necking process is becoming a common practice as a complementary technique for evaluating the extensional properties of low viscosity fluids and for extending the limits of reliable operation for the CaBER™ (Oliveira et al. 2005, 2006; Niedzwiedz et al. 2009, 2010; Roche et al. 2011). Recently, Campo-Deaño and Clasen (2010) presented a reliable technique to measure relaxation times in extension as low as 240 μ s with the CaBER™ using a high-speed camera and a slow retraction method in order to minimize inertial oscillations originated from the acceleration of the liquid. There are also some works where micro-length scales have also been considered with the CaBER™ technique (Kojic et al. 2006; Sattler et al. 2008; Erni et al. 2011) and the range of operation was analyzed theoretically (Ardekani et al. 2010).

In spite of the ability of the filament thinning experiments to stretch significantly the samples, stress measurements indicated that the chains were not reaching their full extension (Babcock et al. 2003). Furthermore, one of the major concerns about filament stretching rheometry is related with the undesirable influence of gravitational effects, since even small gravitational forces can lead to a significant distortion of the liquid bridges (Bänsch et al. 2004).

In recent FiSER™ experiments, the effect of pre-deformation history on the uniaxial extensional flow was analyzed (Anna and McKinley 2008). Recent experiments were carried out in the International Space Station inside the Microgravity Science Glovebox under the auspices of the NASA (SHERE in 2008 and SHERE II in 2011) in order to obtain material property measurements of the fluids using different rotational preshear histories and imposing different axial extensional rates (McKinley and Hall 2011a, b) without the undesirable effects of gravity.

The inherent difficulties of extensional rheometry of low-viscosity fluids due to gravitational and inertial effects can be minimized through miniaturization of rheometric instrumentation. However, the ability of macroscale systems to probe the bulk rheology of a fluid at the microscale remains limited, since the scale down of some mechanical subsystems, such as torsional motors and torque transducers, is impractical (Pipe and McKinley 2009). As an alternative approach, the use of microfluidics for

rheometric purposes is very promising and has attracted the attention of several research groups.

In the present article, we discuss the important recent developments on microfluidic rheometry to generate strong extensional flows and to measure bulk rheological properties in extensional flow, and present a critical assessment of their capabilities and limitations of operation. This review complements the work by Pipe and McKinley (2009), which reviews bulk rheology measurements at the microscale, for shear and extensional flows, but focuses on capillary, stagnation and contraction flows.

2 Microfluidics as a platform for extensional rheometry

Microfluidics is the science and technology of systems that process or manipulate very small amounts of fluids in geometries with characteristic lengthscales ranging from tens to hundreds of micrometres, and is now established as a new field of research (Whitesides 2006). While most research in microfluidics concerns Newtonian fluids, many fluids of interest for lab-on-a-chip applications are likely to exhibit complex microstructure and non-Newtonian behavior, such as viscoelasticity (Squires and Quake 2005). The small characteristic lengthscales of microfluidics enable the generation of flows with high deformation rates while keeping the Reynolds number (Re) small. These unique flow features result in the ability to promote strong viscoelastic effects, quantified by the elasticity number (El) that scales inversely with the square of the characteristic length (L), which are highly enhanced as the scale is reduced. This effect is especially noteworthy for low viscosity complex fluids (e.g. inks, coating fluids, DNA solutions, etc.) (Oliveira et al. 2008b), for which the elasticity number may be small in macroscopic flows ($El \ll 1$), but very large at the microscale and most likely not concealed by flow inertia (Rodd et al. 2005a). Therefore, detailed understanding of the impact of fluid rheological properties on flows at such small scales is clearly desirable. These distinctive flow characteristics together with the development and growth of microfluidic techniques provide a rich platform for rheologists to perform rheometric investigations of non-Newtonian fluid flow phenomena at small scales and new opportunities for material property characterization (Soulages et al. 2009b). Moreover, due to difficulties in the measurement of rheological properties in extensional flows at the macroscopic scale, especially for low viscosity liquids (Petrie 2006; Campo-Deaño and Clasen 2010), the use of microfluidic devices to measure bulk properties in extensional flow is a promising approach and has been an active topic of research in recent years (Pipe and McKinley 2009), examples include microfluidic implementations of the four-roll mill (Lee et al. 2007), the

299 cross-slot flow geometry (Arratia et al. 2008; Alves 2008;
 300 Haward et al. 2012a), or the use of contraction flows (Rodd
 301 et al. 2007; Oliveira et al. 2007a; Campo-Deaño et al.
 302 2011).

303 Based on this scenario, Pipe and McKinley (2009)
 304 reviewed recently that microfluidics can be used to determine
 305 bulk rheological properties of complex fluids, as modern
 306 microrheology does using colloidal probes suspended
 307 in the fluids (Squires and Mason 2010). Moreover,
 308 a microfluidic-based rheometer-on-a-chip has a number of
 309 practical advantages such as having no air–liquid interface,
 310 that might be of interest for use with biological fluids and
 311 fluids prone to evaporation, and additionally it could serve
 312 as an online rheological sensor in many industrial processes
 313 (Bandalusena et al. 2009), which is an important
 314 advantage relative to microrheology. Guillot et al. (2006,
 315 2008) achieved relative success in measuring shear rheo-
 316 logical properties in microfluidic channels. Pipe et al.
 317 (2008) were also able to measure steady shear flow curves
 318 by means of a rheometer-on-a-chip containing three flush
 319 mounted microelectromechanical systems (MEMS) pres-
 320 sure sensors (see Fig. 3), as used in the m-VROC™
 321 microfluidic shear rheometer commercialized by Rheo-
 322 sense Inc. (San Ramon, CA, USA).

323 Summing up, the advent of microfluidic technology has
 324 not only increased the need for rheological information
 325 about diluted polymer solutions but also provided a new
 326 platform for developing and testing new rheometric devi-
 327 ces. In particular, microfluidic stagnation and contraction
 328 flows, used for investigating the longstanding problem of
 329 the extensional behavior of low viscosity viscoelastic liq-
 330 uids, show great potential and are viable alternatives to
 331 conventional rheological characterization techniques.
 332 Additionally, it is a golden opportunity for computational
 333 rheologists to incorporate and test new constitutive

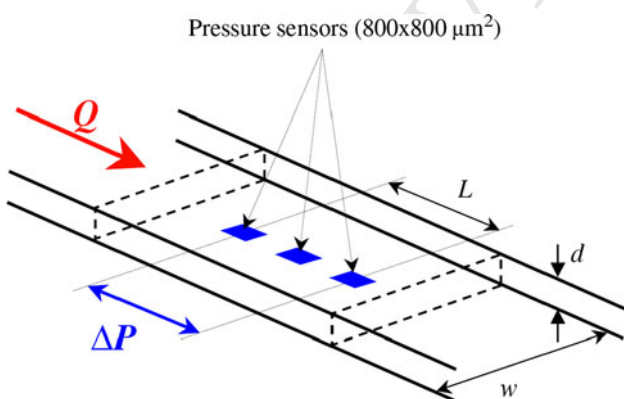


Fig. 3 Illustration of the RheoSense VROC slit microfluidic rheometer, made from Pyrex mounted on a gold-coated silicon substrate with three flush mounted MEMS pressure sensors. With kind permission from Springer Science+Business Media, Pipe et al. (2008, figure 2)

equations for viscoelastic fluid modeling in complex flows, 334
 and investigate high-Weissenberg number flow conditions. 335

2.1 Microfluidic stagnation-point flows

A stagnation-point in a fluid flow is the location where the 337 velocity is zero, but local extension rate can be finite (free 338 stagnation point) or zero (pinned stagnation point) (Soulages 339 et al. 2009b). A classical application of the stagnation-point 340 in fluid flows is the *Pitot tube* used on a routine basis for 341 measuring the flow velocity. Recently, flows with internal 342 (or free) stagnation point, such as those generated 343 in a four-roll mill (Taylor 1934; Lagnado and Leal 1990; 344 Hudson et al. 2004; Pathak and Hudson 2006; Lee et al. 345 2007), cross-slot (Perkins et al. 1997; Remmelgas et al. 346 1999; Arratia et al. 2006; Odell and Carrington 2006; 347 Poole et al. 2007; Alves 2008; Dylla-Spears et al. 2010) or 348 T-junctions (Link et al. 2004; Soulages et al. 2009b), are 349 increasingly popular due to the interest in understanding 350 the flow of complex fluids under strong extensional 351 deformations, and evaluating the extensional properties of 352 dilute polymer solutions in particular (Becherer et al. 353 2008). The vorticity-free state of the flow near a free 354 stagnation-point can result in large extensional deformation 355 and orientation of the microstructure of complex fluids 356 (Pipe and McKinley 2009). Another reason for the interest 357 in stagnation-point flows is their capability to trap macro- 358 molecules or microscopic objects by purely hydrodynamic 359 means while subjecting them to a strong extensional 360 deformation (Tanyeri et al. 2010, 2011), as has been done 361 with long DNA molecules (Shaqfeh 2005; Balducci et al. 362 2008; Dylla-Spears et al. 2010).

Theoretical modeling of stagnation-point flows has 363 proven to be particularly challenging, and despite extensive 364 experimental and theoretical investigation, some aspects of 365 these complex flows remain to be elucidated (Becherer 366 et al. 2008). In the next sections, we focus on the three 367 configurations mostly used in microfluidics for generating 368 stagnation-point flows and we summarize their capabilities 369 and limitations for characterizing extensional properties 370 of low viscosity fluids.

2.1.1 Microfluidic four-roll mill

The *four-roller apparatus* (cf. Fig. 4), commonly known as 374 *four-roll mill*, was invented by Taylor (1934) during his 375 investigations on the stirring process to generate emulsions 376 of two immiscible fluids. This device consists of four 377 cylinders arranged in a square configuration which rotate 378 inside a container filled with fluid. A four-roll mill has the 379 ability to generate different flow kinematics ranging from 380 pure extension, to shear, or to pure rotation, through an 381 appropriate choice of speed and direction of rotation of the 382

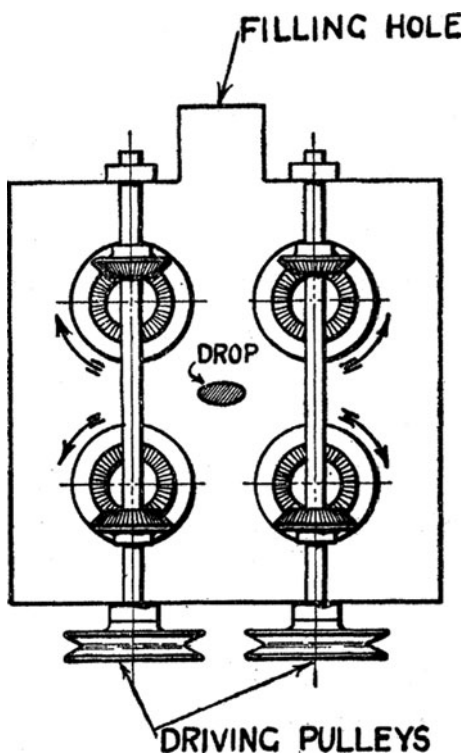


Fig. 4 Original sketch of the “four-roller apparatus”. Reproduced with permission from Taylor (1934)

383 four cylindrical rollers (the apparatus of Fig. 4 is less
384 versatile because the four cylinders cannot be driven
385 independently). Among the wide variety of homogeneous
386 two-dimensional flows that can be produced with a four-
387 roll mill apparatus, the quasi-two-dimensional extensional
388 flow in the central region between the rollers is only one
389 particular case, as highlighted by Lagnado and Leal (1990).
390 Therefore, in principle, combining the capabilities of the
391 four-roll mill and the low inertia flow conditions of mi-
392 crofluidics would offer the possibility of measuring the
393 extensional properties of low viscosity fluids and analyze
394 the response of single molecules under strong extensional
395 flow. However, developing a microfluidic four-roll mill is a
396 challenging task.

397 Hudson et al. (2004) and Phelan Jr. et al. (2005)
398 developed an ingenious microfluidic design of an analog of
399 the four-roll mill, consisting of six intersecting channels
400 with asymmetric configuration (see Fig. 5). By choosing
401 the appropriate flow rate in each channel, they showed that
402 it is possible to create in this geometry a central stagnation
403 point around which the flow type could be varied from pure
404 extension to nearly pure rotation, including simple shear
405 flow conditions (Hudson et al. 2004; Pathak and Hudson
406 2006). However, this microfluidic device has two major
407 drawbacks: pure rotation cannot be obtained due to the
408 asymmetry of the geometry (Lee et al. 2007), and the
409 aspect ratio of the device (depth/width, h/w) must be

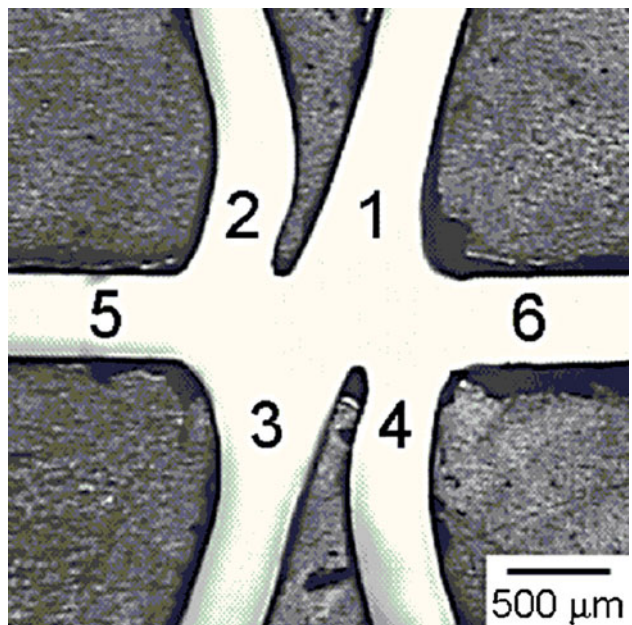


Fig. 5 Microfluidic analog of the four-roll mill proposed by Hudson et al. (2004). Reprinted with permission from Hudson et al. (2004), Copyright (2004), American Institute of Physics

greater than unity to generate substantial rotation (Hudson et al. 2004).

Lee et al. (2007) proposed another microfluidic analogue of a four-roll mill able to keep geometrical symmetry around the stagnation point and to access the full spectrum of flow types, ranging from pure rotation to pure extension, using different aspect ratios of the channel. This microfluidic four-roll mill analogue consists of four inlet and four outlet streams arranged in pairs and disposed symmetrically with regards to the central cavity, as shown in Fig. 6. In comparison with the original design of Hudson et al. (2004), the drawbacks previously mentioned were overcome, since this design is able to achieve pure rotation even with a modest aspect ratio ($h/w \approx 2$), and much lower aspect ratios can be used. Additionally, controlling the flow type becomes easier in this device.

2.1.2 Cross-slot microdevices

Among the microdevices that generate stagnation-point flows, the *cross-slot* device is probably the configuration which has attracted most attention due to its simple geometry and easy control. The standard cross-slot consists of four channels connecting at the same point, arranged orthogonally in the same plane, as illustrated in Fig. 7. The channels can have square, rectangular or circular cross-sections and the space in the chamber can vary in different configurations. When the fluid is injected in two opposing channels at the same flow rate, the opposing fluid streams

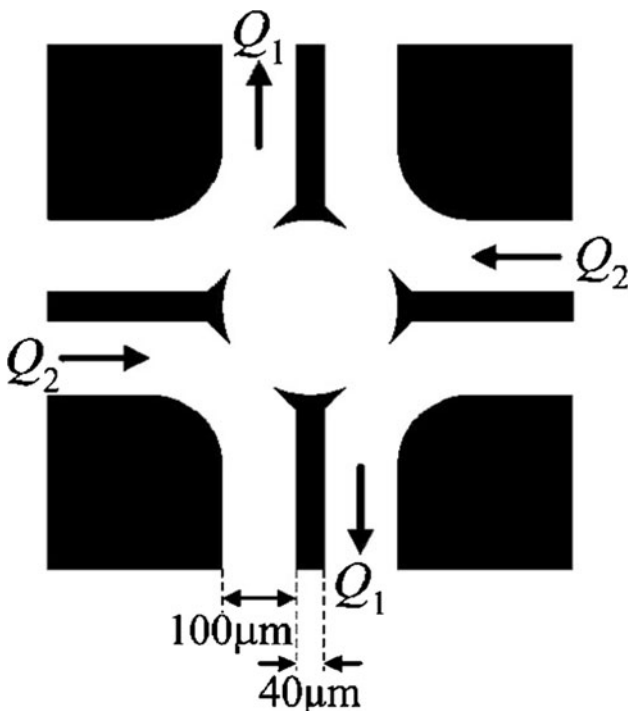


Fig. 6 Schematic diagram of a microfluidic four-roll mill device. Varying the flow rate ratio Q_2/Q_1 allows to generate all flow types. Reprinted with permission from Lee et al. (2007), Copyright (2007), American Institute of Physics

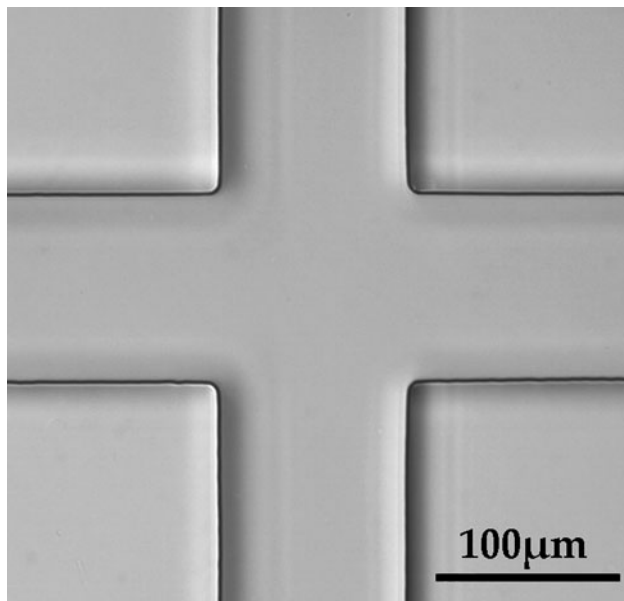


Fig. 7 Bright field image of a standard cross-slot microchannel

437 collide to produce a well-defined stagnation point located
438 at the center of the geometry (if the exit flow rates are also
439 the same), and a strong planar extensional flow is produced
440 in the orthogonal direction while the fluid exits the chamber.
441 Due to these flow characteristics, the standard cross-
442 slot has been used to trap and stretch single molecules, as

done by Dylla-Spears et al. (2010) who investigated the behavior of double-stranded genomic DNA for detection of target sequences along the DNA backbone. The cross-slot microdevice has also been used for analyzing elastic instabilities of polymeric solutions in a planar extensional flow (Arratia et al. 2006; Haward et al. 2012a), which can also be used to induce *enhanced mixing* at microscale (Squires and Quake 2005).

Based on the standard cross-slot configuration, Odell and Carrington (2006) proposed the combination of oscillatory flow with a stagnation point extensional flow field to measure the extensional viscosity of low viscosity fluids. Their extensional flow oscillatory rheometer (EFOR), shown in Fig. 8, consists of a standard cross-slot cell, where the planar extension is created, having four micro-pumps positioned at the end of each channel. These micro-pumps are driven electronically and can induce any cyclic or constant flow rate profile as required, thus controlling the imposed strain and strain-rate. It is also equipped with pressure transducers in two of its limbs to record flow resistance measurements and thus provide information on the apparent extensional viscosity. In addition, by means of an optical probe to measure birefringence, the flow field stability, microstructure and molecular orientation data can be recorded simultaneously. This opto-microfluidic technique has been used in the characterization of both the shear and the extensional response of low-viscosity polymer solutions (Haward 2010; Haward et al. 2011). Moreover, the oscillatory extensional flow technique has potential applications beyond the measurement of extensional viscosity of low viscosity fluids (Odell and Carrington 2006). For instance, it can be used to investigate thermo-mechanical degradation of polymers, or even model extensional and shear flows occurring in porous media flows in tertiary oil-recovery by means of imposing customized flow profiles. Up to the current date the EFOR seems to be the paradigm of the combination between microfluidics and optical techniques for application in rheometry. Its major limitations are related to the capacity of the piezopumps and the pressure transducers, as well as the size of the cross-slot cell, which define the limits of the scale ranges and resolution for the imposed strain rates, inertial forces (Reynolds number) and pressure drop (Odell and Carrington 2006). We note that in the cross-slot chamber the planar extensional flow is not ideal, due to the shear component introduced by the bounding walls.

Computational rheologists have also shown interest in the cross-slot cell for assessing the performance of constitutive models, through comparison with experimental results (Remmelgas et al. 1999), or for gaining insight about purely elastic flow instabilities (Poole et al. 2007). Alves (2008) presented an integrated optimization algorithm able to find an efficient design of the shape of the flow geometry in order

Fig. 8 Illustration of the EFOR set-up. Reprinted from Odell and Carrington (2006), Copyright (2006), with permission from Elsevier Science

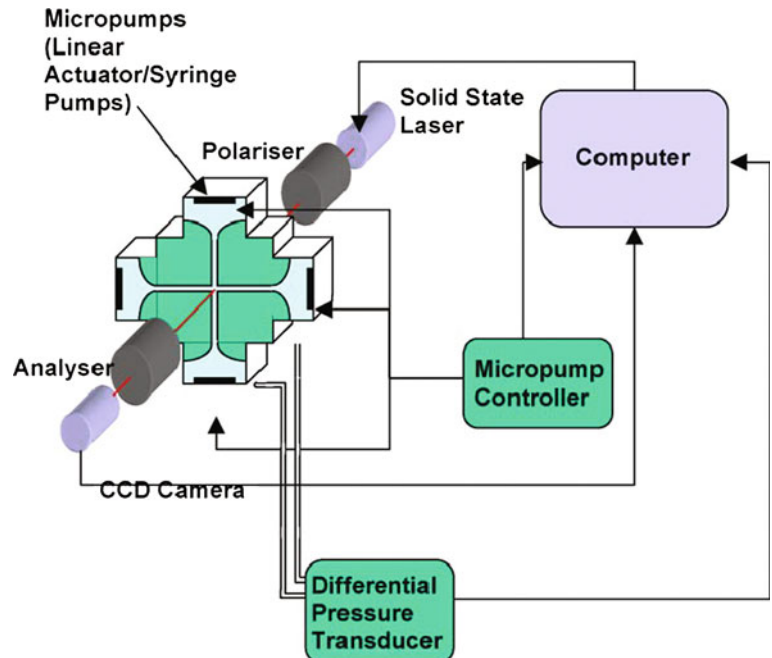
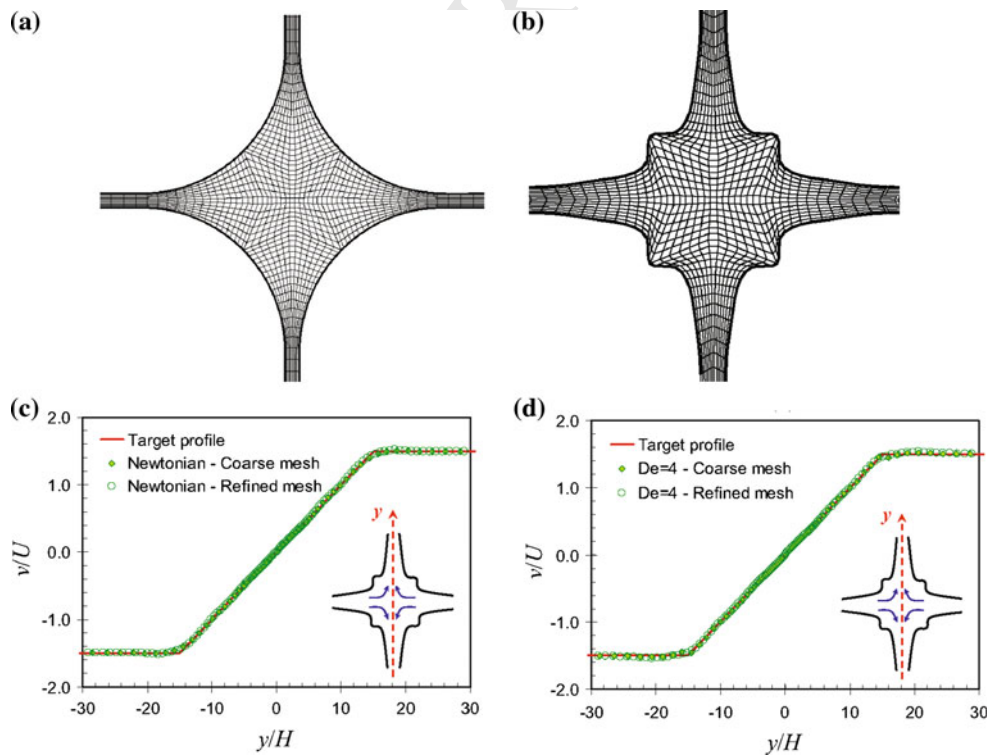


Fig. 9 Illustration of the **a** initial flow configuration, **b** the optimized flow geometry obtained using an optimal shape design technique and **c, d** the numerically predicted velocity profiles along the vertical centerline for Newtonian and viscoelastic fluids. Reprinted with permission from Alves, (2008), Copyright (2008), American Institute of Physics



496 to achieve optimal performance. The standard two-dimensional cross-slot with rounded corners was used by Alves
497 (2008) as initial guess and the optimal shape of the chamber
498 was determined in order to obtain an ideal planar extensional
499 flow along the flow centerlines (see Fig. 9). Recently, the
500 optimized microfluidic device was shown to achieve a quasi-
501 homogeneous elongational flow, a crucial requirement to
502

503 produce meaningful rheological measurements (Haward
504 et al. 2012b).

2.1.3 T-shaped microchannels

505 T-shaped microchannels have been used for multiple purposes,
506 including the generation of micro-droplets in
507

Fig. 10 Comparison of experimental pathlines and numerical simulations (blue solid lines) using the simplified Phan-Thien-Tanner (sPTT) for the microchannels **a** with and **b** without cavity under the same flow conditions. Reprinted from Soulages et al. (2009b), Copyright (2009), with permission from Elsevier Science (color figure online)

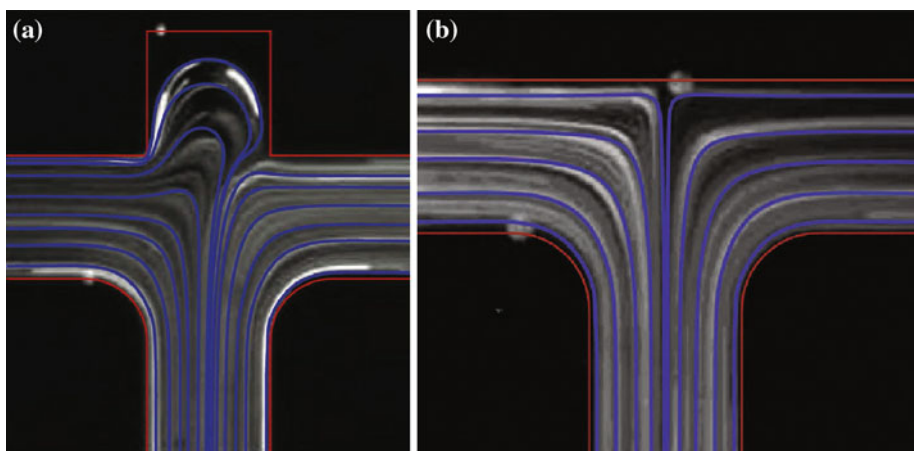
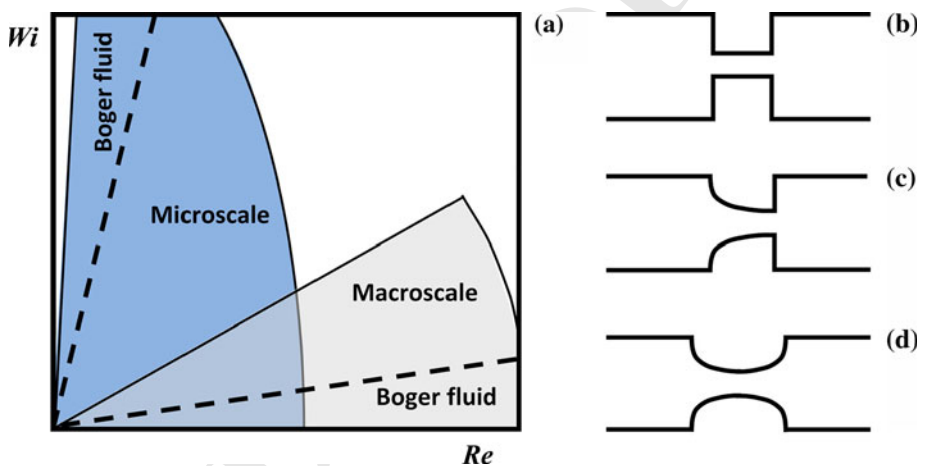


Fig. 11 **a** Operational regions in the Wi - Re parameter space and **b-d** sketch of several canonical contraction-expansion arrangements investigated at the microscale using complex fluids Adapted from Oliveira et al. (2012)



508 microfluidic devices (Husny and Cooper-White 2006), the
509 study of elastic driven instabilities (Soulages et al. 2009b),
510 and for use as passive micro-mixers (Hsieh and Huang 2008).
511 Soulages et al. (2009b) used two distinct T-shaped micro-
512 channels (with and without a small cavity), as illustrated in
513 Fig. 10, to investigate the onset of elastically driven flow
514 asymmetries in steady strong extensional flows. Numerical
515 computations and experiments using streak-imaging and
516 micro-particle image velocimetry (μ PIV) with the T-shaped
517 microchannels showed good agreement and allowed to gain
518 insights about the influence of kinematics near the stagnation
519 point in the resulting polymeric stress fields, and control the
520 critical conditions and spatio-temporal dynamics of the
521 resulting viscoelastic flow instabilities. Despite the partial
522 success in the simulation of complex fluid flow in T-shaped
523 microchannels, their use for the characterization of exten-
524 sional properties of low viscosity fluids is still unexplored.

525 2.2 Microfluidic contraction-expansion flows

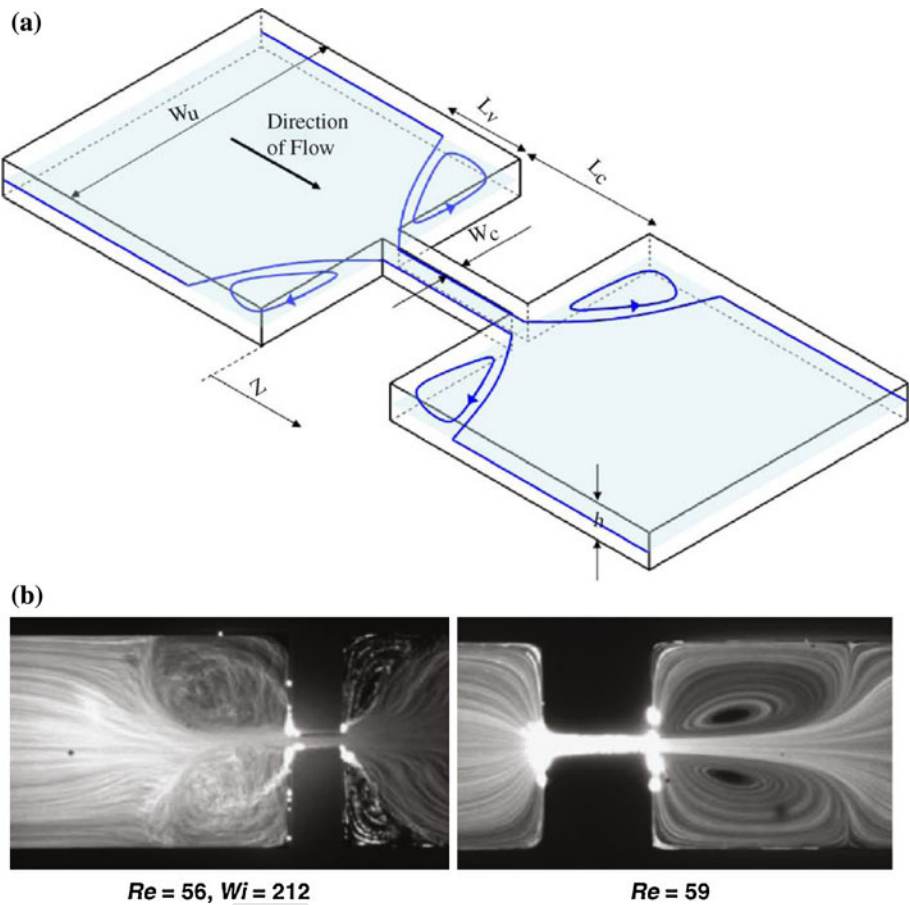
526 Even though flows of complex fluids in converging-diverg-
527 ing microdomains may differ from their counterparts at
528 macroscale there is a common feature: it is a complex flow

containing shear-dominated regions near the walls and non-homogeneous extension along the centerline, with a positive strain rate upstream of the contraction plane and a negative strain rate downstream of the expansion (Rothstein and McKinley 1999, 2001). In the pursuit of developing an efficient microfluidic rheometer-on-a-chip, capable of achieving high strain rates in such a way that it can be used to measure the extensional properties of low viscosity complex fluids, the use of a microfabricated geometry containing a contraction-expansion section is becoming a classical approach after the pioneering works of Rodd et al. (2005a, 2007). At the microscale the small characteristic length-scales enhance the elasticity of the flow ($El = Wi/Re = \frac{\lambda\eta}{\rho L^2}$) and allow to reach unexplored regions in the Weissenberg number – Reynolds number ($Wi - Re$) parameter space, as shown in Fig. 11a (Rodd et al. 2007; Oliveira et al. 2012). In this section, we review the microfluidic contraction-expansion microgeometries frequently used in the characterization of extensional properties of low viscosity fluids, which are illustrated in Fig. 11b–d.

Abrupt contraction-expansion geometries have been used extensively to investigate non-linear flow phenomena associated with fluid elasticity in converging flows at the

529
530
531
532
533
534
535
536
537
538
539
540
541
542
543
544
545
546
547
548
549
550
551

Fig. 12 **a** Schematic diagram of the planar microfluidic contraction-expansion. **b** Comparison between Newtonian (right) and viscoelastic (left) planar entry flows at similar Re in a 16:1 contraction-expansion (flow is from left to right). Reprinted from Rodd et al. (2005a), Copyright (2005), with permission from Elsevier Science



macroscale. However, as previously mentioned, at macro-lengthscales it is not possible to characterize the extensional properties of low viscosity dilute polymer solutions with relaxation times of the order of milliseconds due to the small relative importance of elastic stresses compared to inertial stresses, leading to low values of the elasticity number. However, at the microscale, the elasticity number for the same fluid is much larger and it is possible to observe elastic effects in the flow patterns imaged using streak photography (Rodd et al. 2005a). Figure 12 illustrates the formation of vortices upstream of a microfluidic planar contraction, a well-known feature of viscoelastic fluid flows (Bird et al. 1987). Furthermore, elasticity damps the formation of inertia-driven downstream vortices (Oliveira et al. 2007b; Sousa et al. 2011). Moreover, from a rheometric point of view, this geometry allows for the control of the strain rate by changing the flow rate (Oliveira et al. 2008b).

The ability to determine the excess pressure drop across the contraction-expansion suggests that these devices can be used to develop microfluidic extensional rheometers (Rodd et al. 2005a). However, the flow disturbance induced by the presence of the pressure taps introduced at the channel walls can lead to important errors in the

pressure drop measurements, an effect that is known as the pressure-hole error (Tanner 1988). To overcome this problem, pressure sensors embedded in the surface of the channels could be used as in the Rheosense VROCTM (Pipe et al. 2008). Another drawback of using the abrupt contraction-expansion geometry as a microfluidic extensional rheometer is that the strain rate along the centerline is not constant. In order to minimize this limitation, a more interesting configuration would be a contraction-expansion with a hyperbolic shape, as shown in Fig. 13. The use of hyperbolic contractions results in a quasi-homogeneous extensional flow within the central part of the contraction geometry, and the total Hencky strain experienced by a fluid element is given by $\epsilon_H = \ln(D_1/D_2)$, where D_1 and D_2 are the widths of the large and narrow sections of the hyperbolic contraction, respectively. Higher Hencky strains lead to wider regions of *constant* strain rate in the center of the contraction, although entrance and wall effects are not totally avoided (Oliveira et al. 2007a).

Recently, Campo-Deaño et al. (2011) assessed the capabilities of using an hyperbolic contraction-abrupt expansion geometry as an extensional microrheometer. The relaxation times of low viscosity Boger fluids were estimated by means of the critical Deborah number for the

Fig. 13 Flow patterns for a 50 ppm polyacrylamide aqueous solution with 1 % NaCl at different flow rates. The flow direction is from left to right at the Reynolds and Deborah numbers indicated. Reprinted from Campo-Deaño et al. (2011), Copyright (2011), with permission from Elsevier Science

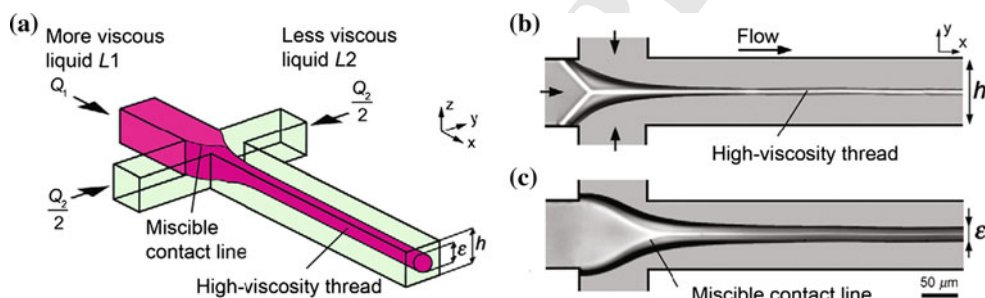
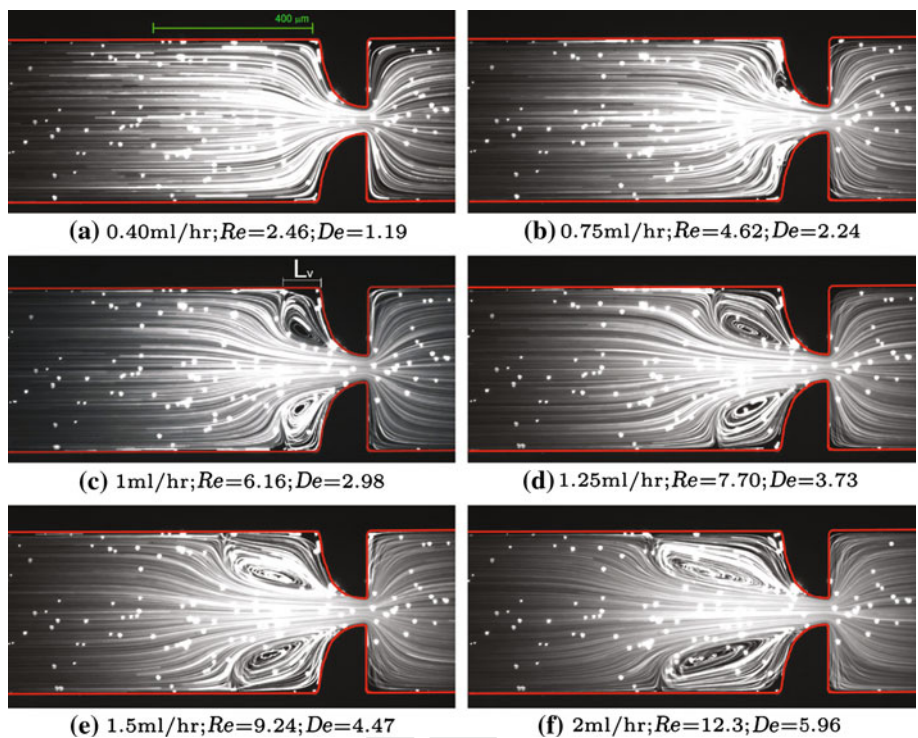


Fig. 14 Formation of threads of a core fluid lubricated with a miscible fluid. **a** Schematic three-dimensional view, **b, c** experimental micrographs of miscible contact lines for different flow rate ratios

onset of secondary flow upstream of the contraction plane, which is assumed to be only weakly dependent on the polymer concentration, at least when inertial effects are negligible (see Fig. 13). One important limitation is that this microgeometry is only suitable for Boger-like fluids, since the presence of shear thinning behavior would make the analysis more complex and eventually trigger the onset of secondary flow downstream of the expansion plane.

608 2.3 Microfluidic flow focusing devices

609 In microfluidic flow focusing devices the shear effects
610 occurring at the walls can be minimized by introducing a
611 lubricating sheath fluid allowing to obtain a shear-free
612 elongational flow on the core fluid, as illustrated in Fig. 14.
613 In this section, we review different geometrical

($\phi = Q_1/Q_2$): **b** $\phi = 0.01$, **c** $\phi = 0.20$. Reprinted from Cubaud and Mason (2009). Copyright (2009), with permission from IOP Publishing Ltd

614 configurations used in flow focusing devices with appli-
615 cation in extensional rheometry, highlighting two key
616 aspects for the success in the development of an exten-
617 sional microrheometer: the miscibility between the fluids
618 and the geometrical shape of the microfluidic device.

619 The miscibility between the core and the lubricating
620 fluids is a crucial parameter to take into account when the
621 working fluids are different. When the fluids are miscible,
622 the lubricating fluid encapsulates the core fluid producing a
623 thread, as shown in Fig. 14a. From the perspective of
624 developing an extensional microrheometer using a flow
625 focusing device, this is very interesting, since the lubricant
626 fluid wraps around the core fluid and forms a thread that
627 fully detaches from the bounding walls, generating a truly
628 shear-free uniaxial extension, neglecting the shear in the
629 interface between both fluids, which is a reasonable



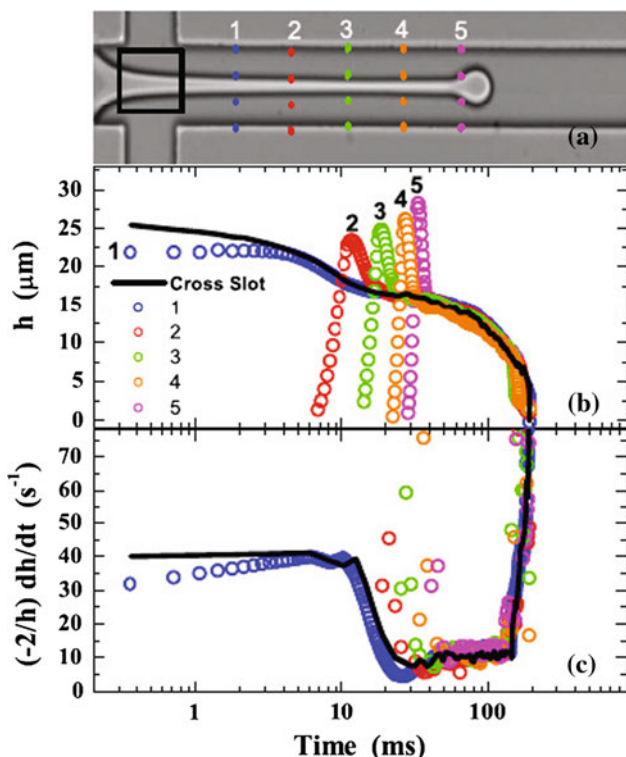


Fig. 15 **a** Filament thickness of a polyacrylamide solution, $h(t)$, measured at different locations in the cross-slot microchannel. A mineral oil is used as lubricating fluid. Measurements are performed in the central region (*square*) and at (*dashed*) lines 1–5. **b** Filament thickness of the polymeric solution at a constant flow rate measured at different locations. Data color is shown in **a**. **c** Computed extensional strain rate, $\dot{\epsilon}$, for the cases illustrated in **b**. The data show that the measurements of $h(t)$ are nearly independent of axial position, after an initial transient period. Reprinted with permission from Arratia et al. (2008). Copyright by the American Physical Society (color figure online)

approximation for low viscosity lubricating fluids. There is an optical signature of the thread encapsulation given by the presence of steady-state miscible contact lines, as shown in Fig. 14b, c. The encapsulation of the core fluid occurs for viscosity ratios above 15 (Cubaud and Mason 2009), when the core fluid is more viscous. When the lubricating and core fluids are immiscible, a different type of thread is formed, and the core fluid remains attached to the top and bottom walls. In this situation, the shear effects from the lateral walls are reduced and a quasi-2D flow representative of planar extensional flow is generated.

Arratia et al. (2008) used a standard cross-slot geometry to induce the stretch of viscoelastic fluids using an immiscible sheath fluid. By means of controlling the ratio between the flow rate of the core and the lubricating fluids ($q = Q_{\text{lub}}/Q_{\text{core}}$) they were able to generate filaments of the core fluid and analyzed the influence of viscoelasticity on filament thinning and breakup, as shown in Fig. 15. The

time evolution of the thickness of the filament, $h(t)$, at the mid-plane of the microchannel ($z = H/2$) was recorded and the extensional strain rate was calculated as $\dot{\epsilon} = -(2/h) \frac{dh}{dt}$.

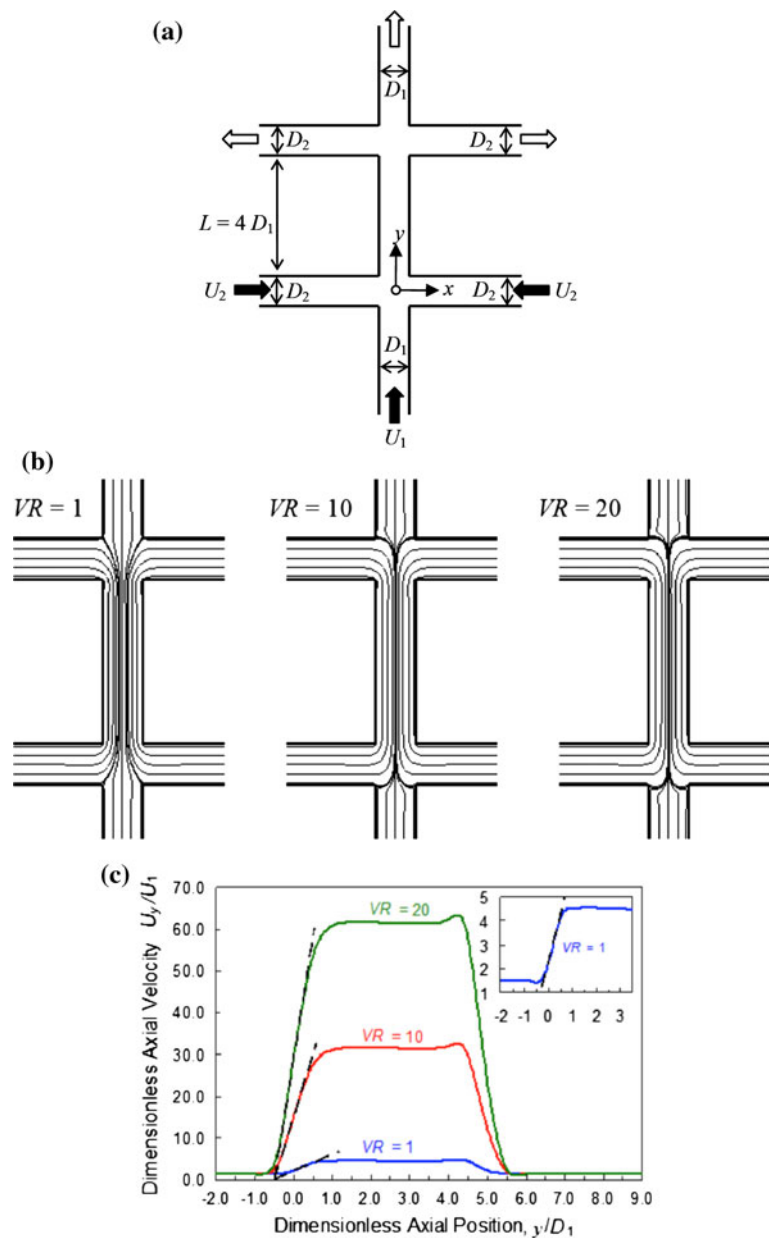
Their results suggest that the steady-state extensional viscosity can be estimated from the exponential rate of thinning. In spite of this breakthrough, one must take into account two key features for having success in the measurement of the steady-state extensional viscosity of the core fluid using this technique:

- The generated filament of the core fluid is not a thread, as occurs in the CaBER but rather a sheet (Cubaud and Mason 2009) having the height of the channel and a thickness that varies ideally only with time. However, depending on the interfacial tension between the core and the lubricating fluids, the thickness can also vary throughout the depth of the channel.
- The depth of the microchannel is also an important parameter, since the top and bottom walls of the microchannels influence the kinematics of the flow at the mid-plane. If the aspect ratio of the channel (depth/width) is not sufficiently large, it is not possible to achieve a shear-free flow at the mid-plane.

In pursuing the understanding of the interplay between viscoelasticity and surfactant dynamics in thread formation and stretching processes in a flow focusing microdevice, Lee et al. (2011) analyzed the ability of viscoelasticity to enhance the formation of jets and long threads. Their analysis focused on the control of droplet formation in flow focusing microdevices, but also showed up to what extent relaxation times extracted from thread formation depend on interfacial properties between the two fluids, which influence the thread formation and breakup mechanisms and may lead to mismatching results.

The double-cross-slot, used by Oliveira et al. (2008a), is another promising approach to generate a shear-free extensional flow with nearly constant strain rate. This device consists of three entrances and three exits disposed in a symmetric configuration, as illustrated in Fig. 16a. By means of numerical calculations, Oliveira et al. (2008a) analyzed the effect of velocity ratio ($VR = U_2/U_1$, where U_1 and U_2 are the inlet average velocities of the core and lubricating fluids, respectively), geometric parameter ($WR = D_2/D_1$) and Deborah number ($De = \lambda U_1/D_1$) on the flow patterns and velocity field for creeping flow conditions in two-dimensional geometries. In Oliveira et al. (2009), a similar flow focusing device with three entrances and a single exit is also analyzed numerically. One advantage of the double cross-slot is that the Hencky strain can be adjusted by varying either VR or WR, since $\epsilon_H = \ln[3(1 + 2VR \times WR)/2]$, and varying VR is straightforward and does not require any change to the microchannel. In this way, using

Fig. 16 **a** Sketch of the double cross-slot geometry. **b** Influence of velocity ratio (VR) on the flow patterns and **c** the axial velocity profiles along the centerline for $D_1 = D_2$ and $De = 0.2$. Reprinted with permission from Oliveira et al. (2008a), Copyright (2008), American Institute of Physics

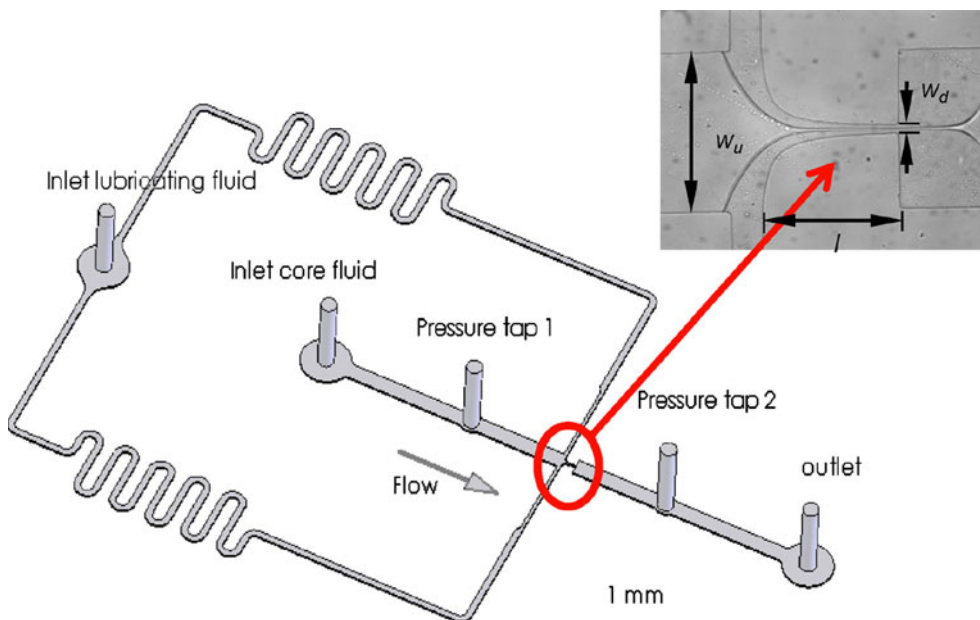


701 only one general device the user can analyze the extensional
702 flow for a range of ϵ_H . Obviously, things are more complex in
703 practice, since the effect of the top and bottom walls has to be
704 taken into consideration, and that inertia might not be neg-
705 ligible for large flow rates. However, this technique for
706 generating extensional flows in microchannels has a great
707 potential despite the lack of published experimental works
708 up to date. This is, undoubtedly, an interesting and relevant
709 area for future research.

710 Recently, Wang and James (2011) proposed an exper-
711 imental technique to estimate the extensional viscosity of
712 dilute polymer solutions as a function of the strain rate
713 using flow in a lubricated, converging microchannel. This
714 apparent extensional viscosity is calculated from the

715 difference between the measured pressure drop and the
716 calculated pressure drop that would occur only due to shear
717 effects in the core flow. The microdevice used consists of a
718 central channel conducting the core fluid, which is con-
719 nected with two side streams containing the lubricating
720 fluid. The fluids then flow through a hyperbolic contraction
721 and an abrupt expansion, as shown in Fig. 17. The authors
722 analyzed the effect of miscibility of the lubricating fluid,
723 and they concluded that flow stability relies on using an
724 immiscible lubricant, which is crucial for assessing fluid
725 resistance to extensional deformation. This technique is
726 also promising as a microfluidic extensional rheometer
727 suitable for characterizing a wide range of weakly elastic
728 fluids.

Fig. 17 Schematic of the lubricated hyperbolic microchannel. The *inset* picture shows a viscous Newtonian fluid lubricated by water introduced through the lateral inlets. Reprinted with permission from Wang and James (2011), Copyright (2011), American Institute of Physics for the Society of Rheology



729 2.4 Electrowetting-on-dielectric microfluidic actuators

730 More than one century after the groundbreaking work in
 731 electrocapillarity by Lippmann (1875), who discovered that
 732 the capillary depression of mercury in contact with elec-
 733 trolyte solutions could be varied by changing the applied
 734 voltage between the mercury and the electrolyte (Mugele
 735 and Baret 2005), the “Electrowetting” effect was described
 736 by Beni and Hackwood (1981) with a practical application
 737 in the development of passive displays. In order to over-
 738 come the problem of electrolysis upon applying voltages
 739 beyond a few millivolts, Berge (1993) proposed to cover
 740 the metallic electrode with a thin insulate layer, which gave
 741 place to the concept of Electrowetting-on-dielectric
 742 (EWOD). Its application to microfluidics is based on the
 743 actuation of tiny amounts of liquids using the principle of
 744 modulating the interfacial tension between a liquid and an
 745 electrode coated with a dielectric layer. When the electric
 746 field is applied only to a portion of the droplet, an imbal-
 747 ance of interfacial tension is created, which forces the
 748 droplet to move (Pollack et al. 2010). Droplets are usually
 749 sandwiched between two parallel plates: the electrode array
 750 is located at the bottom plate, while the top surface is either
 751 a continuous ground plate or a passive top plate (Song
 752 et al. 2009). EWOD has become a widely used concept in
 753 various microfluidic operations including the actuation,
 754 formation, splitting, and mixing of droplets on smooth
 755 surfaces (Kumari and Garimella 2011).

756 The potential of using EWOD actuation in rheometry was
 757 demonstrated by Lin et al. (2007), who proposed a micro-
 758 viscometer based on electrowetting-on-dielectric, and Ban-
 759 purkar et al. (2009), who used EWOD to determine the
 760 elastic moduli of gelled aqueous droplets by using a sessile

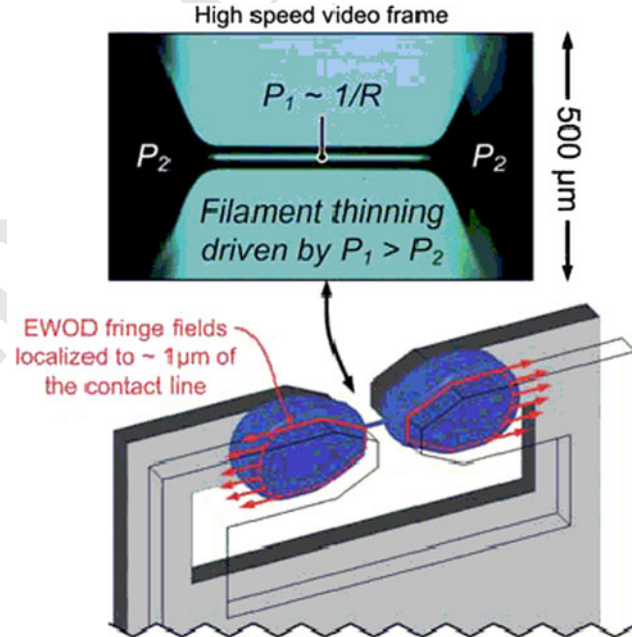


Fig. 18 Three-dimensional sketch of a loaded chip and close-up of the liquid bridge formed using EWOD activation. Reprinted with permission from Nelson et al. (2011), Copyright (2011), The Royal Society of Chemistry

761 droplet and relating liquid properties (e.g. elastic modulus) to
 762 the voltage-dependent measured contact angle. More
 763 recently, Nelson et al. (2010, 2011) went a step forward and
 764 proposed the equivalent of a miniaturized CaBER™ based
 765 on EWOD. Instead of miniaturizing the existing actuators,
 766 they took advantage of the favorable scaling of surface forces
 767 at the microscale and EWOD actuation to avoid using
 768 moving parts. Thus, depending on their electrical properties,
 769 the test samples are pulled by EWOD effects which stretch

770 the droplet as shown in Fig. 18, similar to the way in which
 771 the CaBER™ uses linear actuators to impose a step strain
 772 extending the liquid bridge.

773 This EWOD extensional rheometer exhibits the fol-
 774 lowing advantages:

- 775 776 777 778 779 780 781 782 783 784 785 786 787 788 789 • the undesired oscillations of the suspended fluid induced by inertia are minimized, as the test platform handles tiny sample volumes (Kojic et al. 2006),
- the apparatus is able to easily generate shear-free fluid filaments by either spontaneous capillary wetting or using EWOD actuation. In this scheme, the capillary breakup of a viscoelastic filament is driven by Laplace pressure, and opposed by internal shear and elasticity, without the influence of gravity or inertial-driven oscillations. Therefore, it is possible to measure complex fluids' properties using the known models resulting from a balance of these dominant forces (Nelson et al. 2010),
- the shape of the sample holding platform can be designed in order to facilitate the necking process and to ensure

790 that the measurement point (i.e., the location of the
 791 minimum radius of the filament) remains fixed in space
 792 (Nelson et al. 2010), which is an advantage with regards
 793 to the design of the original CaBER™ system and

- 794 • the micro-machined chip can be easily fabricated and
 795 can be scaled down to handle sub-microliter volumes,
 796 making it especially useful for characterizing expensive
 797 materials and scarce biological fluids.

798 However, the instrument has also some limitations, such as:

- 799 • the applied voltages might influence the rheological
 800 properties of the fluid,
- the length of the initial filament is fixed for each chip,
 801 and may not be appropriate for all kinds of fluids and
 802 • the pre-deformation history cannot be properly controlled.

803 2.5 Surface acoustic wave-induced fluid jetting

804 Tan et al. (2009) demonstrated experimentally that it is
 805 possible to generate a liquid jet ejecting up to 1–2 cm
 806

Fig. 19 **a** Set-up to generate the focused SAWs whose radiation into the drop placed on the substrate focal point induces a deformation into a coherent elongated jet as shown in **b–d**. The water-air interface reflects the acoustic radiation throughout the vertical fluid column as illustrated in **d**. Reprinted with permission from Tan et al. (2009). Copyright (2009) by the American Physical Society

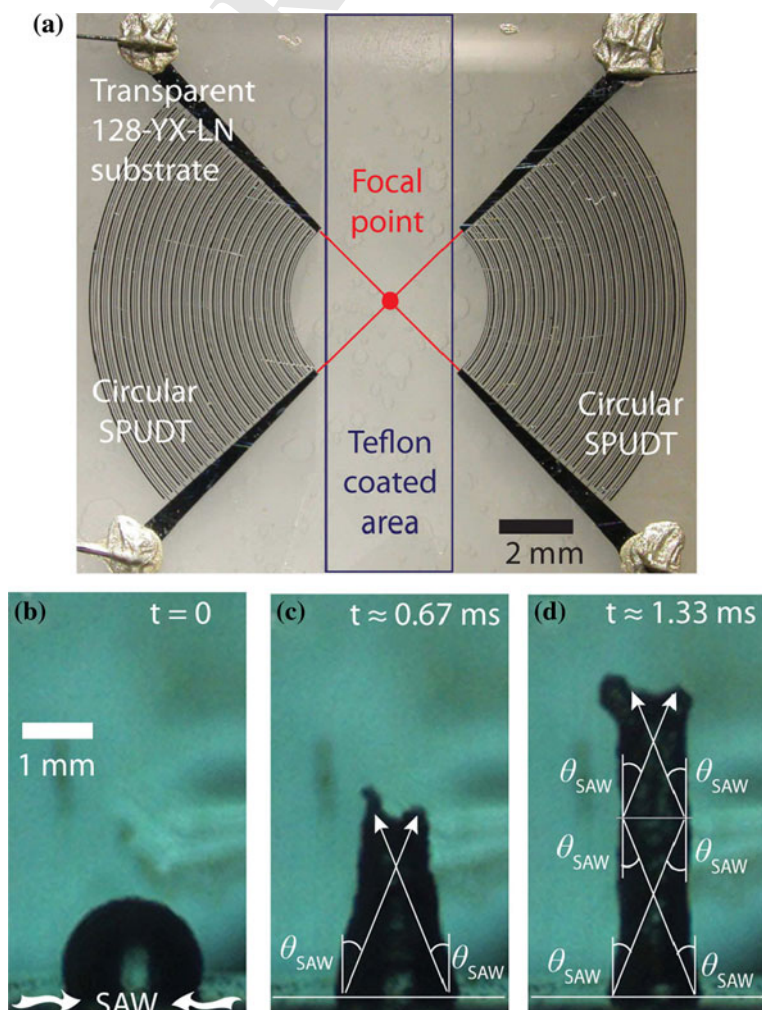
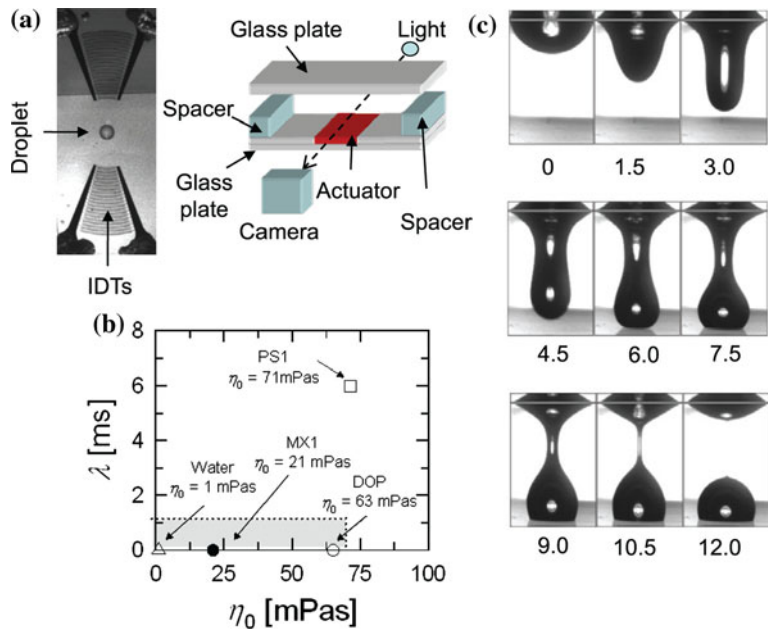


Fig. 20 **a** Set-up for SAW jetting. **b** The solutions used by Bhattacharjee et al. (2011) are shown as symbols. The shaded region in the $\lambda-\eta_0$ parameter space is difficult to access in conventional CaBER™ experiments. **c** Jet formation from the droplet and bridge necking down under the influence of capillary forces acting at the interface. The numbers correspond to the elapsed time in milliseconds. Reprinted from Bhattacharjee et al. (2011), Copyright (2011), with permission from IOP Publishing Ltd



from the free surface of a sessile drop by concentrating the energy of surface acoustic waves (SAW) into the mentioned drop (cf. Fig. 19). Based on this phenomenon, Bhattacharjee et al. (2011) were able to investigate the extensional flow of low-viscosity fluids in capillary bridges formed by pulsed surface acoustic wave jetting. Focusing electrodes at the ends of a lithium niobate piezoelectric crystal provided a focused SAW into the drop placed on the substrate at the focal point, generating a deformation in the form of a coherent elongated jet (left panel of Fig. 20). Using this principle, a liquid bridge can be created when the resulting jet touches and attaches to the top end-plate. In the experiments of Bhattacharjee et al. (2011), the setup was inverted and the droplet jet moved downwards along the direction of gravity. Figure 20c shows the time evolution of the coherent jet formed from the droplet and creation of the liquid bridge. For rheometric measurements the start time is $t_0 = 7.5$ ms, the time at which the SAW actuation ends for the experiment illustrated in Fig. 20c. Subsequently, the bridge thins under the influence of capillary forces acting at the interface. The relaxation time for different fluids are shown in Fig. 20b, illustrating that reliable measurements of Newtonian and viscoelastic fluids can be obtained in the region where the conventional CaBER™ apparatus cannot be used (grey area in Fig. 20b) due to inertia-driven oscillations, with the added advantage of using a small amount of liquid ($\leq 5 \mu\text{l}$). However, the major drawback of this technique lies on the complex combination of operating variables (aperture of the SAW interdigital transducer, contact angle of the fluid, amplitude of the induced SAW and alignment of the end-plates) that must be properly controlled to significantly enhance

the reproducibility of the breakup time of liquid bridges. Without due care, the droplet can fail to jet and form a liquid bridge or even atomize.

3 Perspectives

In this review, we discuss recent advances in microfluidic techniques relevant for the development of an extensional rheometer-on-a-chip able to characterize the extensional properties of low viscosity elastic fluids. In recent years, microfluidics has evolved from being a promising platform for rheometry to becoming one of the most suitable approaches in the characterization of extensional properties of dilute polymer solutions at the moment. However, despite the great progresses, there is still much to be done in order to improve current techniques and, of course, there are also many unexplored approaches to be pursued. In designing and optimizing a microfluidic geometry it is desirable to combine experiments with numerical computations of the corresponding flow field in order to achieve an ideal flow field and systematically explore the sensitivity of the kinematics to changes in the geometry and the flow conditions. This is arguably the best approach to proceed in order to succeed in the quest of designing efficient microfluidic extensional rheometers with optimal performance.

Acknowledgments The authors would like to acknowledge Fundação para a Ciência e a Tecnologia (FCT), COMPETE and FEDER for financial support through projects PTDC/EME-MFE/099109/2008, PTDC/EME-MFE/114322/2009, PTDC/EQU-FTT/118716/2010 and the scholarship SFRH/BPD/69663/2010. The authors also thank Dr. Rob Poole (University of Liverpool) for helpful comments.

870

References

- Alves MA (2008) Design a cross-slot flow channel for extensional viscosity measurements. AIP Conf Proc 1027:240–242
- Anna SL, McKinley GH (2008) Effect of a controlled pre-deformation history on extensional viscosity of dilute polymer solutions. *Rheol Acta* 47:841–859
- Anna SL, Rogers C, McKinley GH (1999) On controlling the kinematics of a filament stretching rheometer using a real-time active control mechanism. *J Non Newton Fluid Mech* 87:307–335
- Anna SL, McKinley GH, Nguyen DA, Sridhar T, Muller S, Huang J, James DF (2001) An interlaboratory comparison of measurements from filament-stretching rheometers using common test fluids. *J Rheol* 45(1):83–114
- Ardekani AM, Sharma V, McKinley GH (2010) Dynamics of bead formation, filament thinning and breakup in weakly viscoelastic jets. *J Fluid Mech* 665:46–56
- Arratia PE, Thomas CC, Diorio J, Gollub JP (2006) Elastic instabilities of polymer solutions in cross-channel flow. *Phys Rev Lett* 96:144502
- Arratia PE, Gollub JP, Durian DJ (2008) Polymeric filament thinning and breakup in microchannels. *Phys Rev E* 77:036309
- Babcock HP, Teixeira RE, Hur JS, Shaqfeh ESG (2003) Visualization of molecular fluctuations near the critical point of the coil-stretch transition in polymer elongation. *Macromolecules* 36:4544–4548
- Baldacci AG, Tang J, Doyle PS (2008) Electrophoretic stretching of dna molecules in cross-slot nanoslit channels. *Macromolecules* 41:9914–9918
- Bandalusena HCH, Zimmerman WB, Rees JM (2009) Microfluidic rheometry of a polymer solution by micron resolution particle image velocimetry: a model validation study. *Meas Sci Technol* 20:115404
- Banpurkar AG, Duits MHG, van den Ende D, Mugele F (2009) Electrowetting of complex fluids: perspectives for rheometry on chip. *Langmuir* 25:1245–1252
- Bänsch E, Berg CP, Ohlhoff A (2004) Uniaxial extensional flows in liquid bridges. *J Fluid Mech* 521:353–379
- Barnes HA, Hutton JF, Walters K (1993) An introduction to rheology. *Rheology series*, 3rd edn. Elsevier, The Netherlands
- Bazilevsky A, Entov V, Rozhkov A (1990) Liquid filament micro-rheometer and some of its applications. In: Oliver DR (ed) *Proceedings of the third European rheology conference*. Elsevier, The Netherlands, pp 41–43
- Becherer P, Morozov AN, van Saarloos W (2008) Scaling of singular structures in extensional flow of dilute polymer solutions. *J Non Newton Fluid Mech* 153:183–190
- Beni G, Hackwood S (1981) Electro-wetting displays. *Appl Phys Lett* 38(4):207–209
- Berge B (1993) Electrocapillarité et mouillage de films isolants par l'eau. *Comptes rendus de l' Academie des sciences Serie 2* 317(2):157–163
- Bhattacharjee PK, McDonnell AG, Prabhakar R, Yeo LY, Friend J (2011) Extensional flow of low-viscosity fluids in capillary bridges formed by pulsed surface acoustic wave jetting. *New J Phys* 13:023005
- Bird RB, Armstrong RC, Hassager O (1987) Dynamics of polymer liquids. *Fluid mechanics*, vol 1, 2nd edn. Wiley, USA
- Campo-Deaño L, Clasen C (2010) The slow retraction method (SRM) for the determination of ultra-short relaxation times in capillary breakup extensional rheometry experiments. *J Non Newton Fluid Mech* 165:1688–1699
- Campo-Deaño L, Galindo-Rosales FJ, Pinho FT, Alves MA, Oliveira MSN (2011) Flow of low viscosity boger fluids through a microfluidic hyperbolic contraction. *J Non Newton Fluid Mech* 166:1286–1296

- Cubaud T, Mason TG (2009) High-viscosity fluids threads in weakly diffusive microfluidic systems. *New J Phys* 11:075029
- Dontula P, Pasquali M, Scriven LE, Macosko CW (1997) Can extensional viscosity be measured with opposed-nozzle devices. *Rheol Acta* 36:429–448
- Dukhin A, Zelenov A (2010) Rheology: shear, extensional, longitudinal. *Sci Topics*. http://www.scitopics.com/Rheology_shear_extensional_longitudinal.html (accessed 20 June 2012)
- Dylla-Spears R, Townsend JE, Jen-Jacobson L, Sohn LL, Muller SJ (2010) Single-molecule sequence detection via microfluidic planar extensional flow at a stagnation point. *Lab Chip* 10:1543–1549
- Erni P, Varagnat M, Clasen C, Crest J, McKinley GH (2011) Microrheometry of sub-nanolitre biopolymer samples: non-newtonian flow phenomena of carnivorous plant mucilage. *Soft Matter* 7:10889
- Franck A (2011) The ARES-EVF: option for measuring extensional viscosity of polymer melts. http://www.tainstruments.com/pdf/literature/APN002_V2_ARES_EVF_to_measure_elongation_viscosity.pdf (accessed 20 June 2012)
- Fuller GG, Cathey CA, Hubbard B, Zebrowski BE (1987) Extensional viscosity measurements for low-viscosity fluids. *J Rheol* 31:235–249
- Funami T (2011) Next target for food hydrocolloid studies: texture design of foods using hydrocolloid technology. *Food Hydrocolloids* 25:1904–1914
- Gaudet S, McKinley GH (1998) Extensional deformation of non-Newtonian liquid bridges. *Comput Mech* 21:461–476
- Göttfert (2011) Elongational testing—rheotens and haul-off. http://www.goettfert.com/images/stories/downloads/produkte_Rheotens_71-97_en.pdf (accessed 20 June 2012)
- Guillot P, Panizza P, Salmon JP, Joanicot M, Colin A (2006) Viscosimeter on a microfluidic chip. *Langmuir* 22:6438–6445
- Guillot P, Moulin T, Kotitz RMG, Dodge A, Joanicot M, Colin A, Bruneau CH, Colin T (2008) Towards a continuous microfluidic rheometer. *Microfluid Nanofluid* 5:619–630
- Gupta RK, Sridhar T (1988) Rheological Measurements. In: Clegg D, Collyer AA (eds) Elsevier, The Netherlands
- Haward SJ (2010) Buckling instabilities in dilute polymer solution elastic strands. *Rheol Acta* 49:1219–1225
- Haward SJ, Odell JA, Berry M, Hall T (2011) Extensional rheology of human saliva. *Rheol Acta* 50:869–879
- Haward SJ, Ober TJ, Oliveira MSN, Alves MA, McKinley GH (2012a) Extensional rheology and elastic instabilities of a wormlike micellar solution in a microfluidic cross-slot device. *Soft Matter* 8:536–555
- Haward SJ, Oliveira MSN, Alves MA, McKinley GH (2012b) Optimized cross-slot flow geometry for microfluidic extensional rheometry. *Phys Rev Lett* (submitted)
- Hermansky CG, Boger DV (1995) Opposing-jet viscometry of fluids with viscosity approaching that of water. *J Non Newton Fluid Mech* 56:1–14
- Hsieh SS, Huang YC (2008) Passive mixing in micro-channels with geometric variations through μ PIV and μ LIF measurements. *J Micromech Microeng* 18:065017
- Hudson SD, Phelan FR, Handler MD, Cabral JT, Migler KB, Amis EJ (2004) Microfluidic analog of the four-roll mill. *Appl Phys Lett* 85(2):335–337
- Husny J, Cooper-White JJ (2006) The effect of elasticity on drop creation in T-shaped microchannels. *J Non Newton Fluid Mech* 137:121–136
- Kojic N, Bico J, Clasen C, McKinley GH (2006) *Ex vivo* rheology of spider silk. *J Exp Biol* 209:4355–4362
- Kumari N, Garimella SV (2011) Electrowetting-induced dewetting transitions on superhydrophobic surfaces. *Langmuir* 27:10342–10346



- 999 Lagnado RR, Leal LG (1990) Visualization of three-dimensional flow
1000 in a four-roll mill. *Exp Fluids* 9:25–32
1001 Lee JS, Dylla-Spears R, Teclamariam NP, Muller SJ (2007)
1002 Microfluidic four-roll mill for all flow types. *Appl Phys Lett*
1003 90:074103
1004 Lee W, Walker LM, Anna SL (2011) Competition between visco-
1005 elasticity and surfactant dynamics in flow focusing microfluidics.
1006 *Macromol Mater Eng* 296:203–213
1007 Lin YY, Lin CW, Yang LJ, Wang AB (2007) Micro-viscometer based
1008 on electrowetting on dielectric. *Electrochim Acta* 52:2876–2883
1009 Link DR, Anna SL, Weitz DA, Stone HA (2004) Geometrically
1010 mediated breakup of drops in microfluidic devices. *Phys Rev Lett*
1011 92(5):054503
1012 Lippmann G (1875) Relations entre les phénomènes électriques et
1013 capillaires. *Ann Chim Phys* 5:494
1014 Macosko CW (1994) Rheology: principles, measurements, and
1015 applications. Wiley, USA
1016 Maia JM, Covas JA, Nóbrega JM, Dias TF, Alves FE (1999)
1017 Measuring uniaxial extensional viscosity using a modified
1018 rotational rheometer. *J Non Newton Fluid Mech* 80:183–197
1019 Matta JE, Tytus RP (1990) Liquid stretching using a falling cylinder.
1020 *J Non Newton Fluid Mech* 35:215–229
1021 McKinley GH (2005) Visco-elasto-capillary thinning and break-up of
1022 complex fluids. In: Binding DM, Walters K (eds) *Rheology reviews*. The British Society of Rheology
1023
1024 McKinley GH, Hall NR (2011a) Shear history extensional rheology
1025 experiment II (SHERE II). http://issresearchproject.grc.nasa.gov/MSG/SHERE_II/ (accessed 20 June 2012)
1026 McKinley GH, Hall NR (2011b) Shear history extensional rheology
1027 experiment (SHERE). <http://issresearchproject.grc.nasa.gov/MSG/SHERE/> (accessed 20 June 2012)
1028 McKinley GH, Sridhar T (2002) Filament-stretching rheometry of
1029 complex fluids. *Annu Rev Fluid Mech* 34:375–415
1030 McKinley GH, Tripathi A (2000) How to extract the Newtonian
1031 viscosity from capillary breakup measurements in a filament
1032 rheometer. *J Rheol* 44(3):653–671
1033 McKinley GH, Brauner O, Yao M (2001) Kinematics of filament
1034 stretching in dilute and concentrated polymer solutions. *Korea
1035 Austral J Rheol* 13(1):29–35
1036 Meissner J (1985a) Experimental aspects in polymer melt elongational
1037 rheometry. *Chem Eng Commun* 33:159–180
1038 Meissner J (1985b) Rheometry of polymer melts. *Annu Rev Fluid
1039 Mech* 17:45–64
1040 Mugele F, Baret JC (2005) Electrowetting: from basics to applica-
1041 tions. *J Phys Condens Matter* 17:R705–R774
1042 Münsted H (1979) New universal extensional rheometer for polymer
1043 melts. Measurements on a polystyrene sample. *J Rheol*
1044 23(4):421–436
1045 Nelson WC, Kavehpour HP, Kim CJ (2010) A micro extensional
1046 filament rheometer enabled by EWOD. In: IEEE 23rd international
1047 conference on micro electro mechanical systems (MEMS), pp 75–78
1048 Nelson WC, Kavehpour HP, Kim CJ (2011) A miniature capillary
1049 breakup extensional rheometer by electrostatically assisted
1050 generation of liquid filaments. *Lab Chip* 11:2424–2431
1051 Ng SL, Mun RP, Boger DV, James DF (1996) Extensional viscosity
1052 measurements of dilute polymer solutions of various polymers.
1053 *J Non Newton Fluid Mech* 65:291–298
1054 Niedzwiedz K, Arnolds O, Willenbacher N, Brummer R (2009) How
1055 to characterize yield stress fluids with capillary breakup exten-
1056 sional rheometry (CaBER). *Appl Rheol* 19(4):41969
1057 Niedzwiedz K, Buggisch H, Willenbacher N (2010) Extensional
1058 rheology of concentrated emulsions as probed by capillary
1059 breakup elongational rheometry (CaBER). *Rheol Acta*
1060 49:1103–1116
1061
1062
1063
Nijenhuis K, McKinley GH, Spiegelberg S, Barnes HA, Aksel N,
1064 Heymann L, Odell JA (2007) Springer handbook on experimen-
1065 tal fluid mechanics, Chap 9. Non-Newtonian flows. Springer,
1066 Berlin
1067 Odell JA, Carrington SA (2006) Extensional flow oscillatory rheo-
1068 metry. *J Non Newton Fluid Mech* 137:110–120
1069 Oliveira MSN, McKinley GH (2005) Iterated stretching and multiple
1070 beads-on-a-string phenomena in dilute solutions of highly
1071 extensible flexible polymers. *Phys Fluids* 17:071704
1072 Oliveira MSN, Yeh R, McKinley GH (2006) Iterated stretching,
1073 extensional rheology and formation of beads-on-a-string struc-
1074 tures in polymer solutions. *J Non Newton Fluid Mech*
1075 137:137–148
1076 Oliveira MSN, Alves MA, Pinho FT, McKinley GH (2007a) Viscous
1077 flow through microfabricated hyperbolic contractions. *Exp
1078 Fluids* 43:437–451
1079 Oliveira MSN, Oliveira PJ, Pinho FT, Alves MA (2007b) Effect of
1080 contraction ratio upon viscoelastic flow in contractions: the
1081 axisymmetric case. *J Non Newton Fluid Mech* 147:92–108
1082 Oliveira MSN, Alves MA, Pinho FT (2008a) Extensional effects in
1083 viscoelastic fluid flow through a micro-scale double cross-slot.
AIP Conf Proc 1027:982–984
1084 Oliveira MSN, Rodd LE, McKinley GH, Alves MA (2008b)
1085 Simulations of extensional flow in microrheometric devices.
1086 *Microfluid Nanofluid* 5:809–826
1087 Oliveira MSN, Pinho FT, Poole RJ, Oliveira PJ, Alves MA (2009)
1088 Purely-elastic flow asymmetries in flow focusing devices. *J Non
1089 Newton Fluid Mech* 160:31–39
1090 Oliveira MSN, Alves MA, Pinho FT (2012) Transport and mixing in
1091 laminar flows: from microfluidics to oceanic currents, Chap 6.
1092 *Microfluidic flows of viscoelastic fluids*. Wiley, New York
1093 Padmanabhan M (1995) Measurement of extensional viscosity of
1094 viscoelastic liquid foods. *J Food Eng* 25:311–327
1095 Padmanabhan M, Bhattacharya M (1993) Planar extensional viscosity
1096 of corn meal dough. *J Food Eng* 18:389–411
1097 Pathak JA, Hudson SD (2006) Rheo-optics of equilibrium polymer
1098 solutions: wormlike micelles in elongational flow in a microflu-
1099 idic cross-slot. *Macromolecules* 39:8782–8792
1100 Perkins TT, Smith DE, Chu S (1997) Single polymer dynamics in an
1101 elongation flow. *Science* 314:216–221
1102 Petrie CJS (1997) Three-dimensional presentation of extensional flow
1103 data. *J Non Newton Fluid Mech* 70:205–218
1104 Petrie CJS (2006) Extensional viscosity: a critical discussion. *J Non
1105 Newton Fluid Mech* 137:15–23
1106 Phelan FR Jr, Hudson SD, Handler MD (2005) Fluid dynamics
1107 analysis of channel flow geometries for materials characteriza-
1108 tion in microfluidic devices. *Rheol Acta* 45:59–71
1109 Pipe C, McKinley GH (2009) Microfluidic rheometry. *Mech Res
1110 Commun* 36:110–120
1111 Pipe C, Majmudar TS, McKinley GH (2008) High shear rate
1112 viscometry. *Rheol Acta* 47:621–642
1113 Pollack MG, Fair RB, Shenderov AD (2010) Electrowetting-based
1114 actuation of liquid droplets for microfluidic applications. *Appl
1115 Phys Lett* 77:1725–1727
1116 Poole RJ, Alves MA, Oliveira PJ (2007) Purely elastic flow
1117 asymmetries. *Phys Rev Lett* 99:164503
1118 Remmelgas J, Singh P, Leal LG (1999) Computational studies of
1119 nonlinear elastic dumbbell models of boger fluids in a cross-slot
1120 flow. *J Non Newton Fluid Mech* 88:31–61
1121 Ríos S, Díaz J, Galindo A, Soto E, Calderas F, Mena B (2002)
1122 Instrumentation and start up of a new elongational rheometer
1123 with preshearing history. *Rev Sci Instrum* 73:3007–3011
1124 Roche M, Kellay H, Stone HA (2011) Heterogeneity and the role of
1125 normal stresses during the extensional thinning of non-Brownian
1126 shear-thickening fluids. *Phys Rev Lett* 107:34503
1127
1128

- 1129 Rodd LE, Scott TP, Boger DV, Cooper-White JJ, McKinley GH
1130 (2005a) The inertio-elastic planar entry flow of low-viscosity
1131 elastic fluids in micro-fabricated geometries. *J Non Newtonian*
1132 *Fluid Mech* 129:1–22
- 1133 Rodd LE, Scott TP, Cooper-White JJ, McKinley GH (2005b)
1134 Capillary break-up rheometry of low-viscosity elastic fluids.
1135 *Appl Rheol* 15:12–27
- 1136 Rodd LE, Cooper-White JJ, Boger DV, McKinley GH (2007) The
1137 role of elasticity number in the entry flow of dilute polymer
1138 solutions in micro-fabricated contraction geometries. *J Non*
1139 *Newtonian Fluid Mech* 143:170–191
- 1140 Rothstein JP (2008) Strong flows of viscoelastic wormlike micelle
1141 solutions. In: Binding DM, Walters K (eds) *Rheology reviews*.
1142 The British Society of Rheology
- 1143 Rothstein JP, McKinley GH (1999) Extensional flow of a polystyrene
1144 boger fluid through a 4:1:4 axisymmetric contraction/expansion.
1145 *J Non Newton Fluid Mech* 86:61–88
- 1146 Rothstein JP, McKinley GH (2001) The axisymmetric contraction–
1147 expansion: the role of extensional rheology on vortex growth
1148 dynamics and the enhanced pressure drop. *J Non Newton Fluid*
1149 *Mech* 98:33–63
- 1150 Sattler R, Wagner C, Eggers J (2008) Blistering pattern and formation
1151 of nanofibers in capillary thinning of polymer solutions. *Phys*
1152 *Rev Lett* 100:164502
- 1153 Schultz WW, Davis SH (1982) One-dimensional liquid fibers. *J Rheol*
1154 26(4):331–345
- 1155 Schweizer T (2000) The uniaxial elongational rheometer rme—six
1156 years of experience. *Rheol Acta* 39:428–443
- 1157 Sentmanat M, Wang BN, McKinley GH (2005) Measuring the
1158 transient extensional rheology of polyethylene melts using the
1159 ser universal testing platform. *J Rheol* 49(3):585–606
- 1160 Shaqfeh ESG (2005) The dynamics of single-molecule dna in flow.
1161 *J Non Newton Fluid Mech* 130:1–28
- 1162 Song JH, Evans R, Lin YY, Hsu BN, Fair RB (2009) A scaling model
1163 for electrowetting-on-dielectric microfluidic actuators. *Micro-*
1164 *fluid Nanofluid* 7:75–89
- 1165 Soulages J, Le Gouip F, Hostettler J, McKinley GH (2009a) An
1166 opposed-nozzle fixture for measuring the extensional properties
1167 of low viscosity liquids using a conventional controlled strain
1168 rheometer. In: Co A (ed) *The Society of Rheology. 81st annual*
1169 *meeting program and abstracts*, p 115
- 1170 Soulages J, Oliveira MSN, Sousa PC, Alves MA, McKinley GH
1171 (2009b) Investigating the stability of viscoelastic stagnation
1172 flows in t-shaped microchannels. *J Non Newton Fluid Mech*
1173 163:9–24
- 1174 Sousa PC, Coelho PM, Oliveira MSN, Alves MA (2011) Laminar
1175 flow in three-dimensional square–square expansion. *J Non*
1176 *Newton Fluid Mech* 166:1033–1048
- 1177 Squires TM, Mason TG (2010) Fluid mechanics of microrheology.
1178 *Annu Rev Fluid Mech* 42:413–438
- 1179 Squires TM, Quake SR (2005) Microfluidics: fluid physics at the
1180 nanoliter scale. *Rev Mod Phys* 77:977–1026
- 1181 Sridhar T (2000) From rheometry to rheology. *Korea Austral Rheol J*
1182 12(1):39–53
- 1183 Tan MK, Friend JR, Yeo LY (2009) Interfacial jetting phenomena
1184 induced by focusing surface vibrations. *Phys Rev Lett*
1185 103:024501
- 1186 Tanner RI (1988) Pressure-hole errors—an alternative approach.
1187 *J Non Newtonian Fluid Mech* 28:309–318
- 1188 Tanyeri M, Johnson-Chavarria EM, Schroeder CM (2010) Hydrody-
1189 namic trap for single particles and cells. *Appl Phys Lett*
1190 96:224101
- 1191 Tanyeri M, Ranka M, Sittipolkul N, Schroeder CM (2011) A
1192 microfluidic-based hydrodynamic trap: design and implemen-
1193 tation. *Lab Chip* 11:1786–1794
- 1194 Taylor GI (1934) The formation of emulsions in definable fields of
1195 flow. *Proc Roy Soc Lond Ser A* 146:501–523
- 1196 Trouton FT (1906) On the coefficient of viscous traction and its
1197 relation to that of viscosity. *Proc Roy Soc Lond* 77:426–440
- 1198 Wang J, James DF (2011) Lubricated extensional flow of viscoelastic
1199 fluid in a convergent microchannel. *J Rheol* 55:1103–1126
- 1200 Whitesides GM (2006) The origins and future of microfluidics.
1201 *Nature* 42:368–370
- 1202 Zheng R, Tanner RI, Fan XJ (2011) *Injection molding: integration of*
1203 *theory and modeling methods*. Springer, Berlin
- 1204

